Clim Dyn (2008) 30:567–579
DOI 10.1007/s00382-007-0308-z

Simulation of the evolutionary response of global summer monsoons to orbital forcing over the past 280,000 years

J. E. Kutzbach · Xiaodong Liu · Zhengyu Liu · Guangshan Chen

Received: 25 April 2007 / Accepted: 23 August 2007 / Published online: 19 October 2007

Abstract We describe the evolutionary response of northern and southern hemisphere summer monsoons to orbital forcing over the past 280,000 years using a fully coupled general circulation ocean-atmosphere model in which the orbital forcing is accelerated by a factor of 100. We find a strong and positive response of northern (southern) summer monsoon precipitation to northern (southern) summer insolation forcing. On average, July (January) precipitation maxima and JJA (DJF) precipitation maxima have high coherence and are approximately in phase with June (December) insolation maxima, implying an average lag between forcing and response of about 30° of phase at the precession period. The average lag increases to over 40° for 4-month precipitation averages, JJAS (DJFM). The phase varies from region to region. The average JJA (DJF) land temperature maxima also lag the June orbital forcing maxima by about 30° of phase, whereas ocean temperature maxima exhibit a lag of about 60° of phase at the precession period. Using generalized measures of the thermal and hydrologic processes that produce monsoons, we find that the summer monsoon precipitation indices for the six regions all fall within the phase limits of the process indices for the respective hemispheres. Selected observational studies from four of the six monsoon regions report approximate in-phase relations of summer monsoon proxies to summer insolation. However other observational studies report substantial phase lags of monsoon proxies and a strong component of forcing associated with glacial-age boundary conditions or other factors. An important next step will be to include glacial-age boundary condition forcing in long, transient paleoclimate simulations, along with orbital forcing.

Keywords Paleoclimate · Monsoons · Orbital cycles · Climate models · Transient simulations

J. E. Kutzbach (✉) · Z. Liu · G. Chen
Center for Climatic Research,
University of Wisconsin-Madison,
1225 West Dayton St, Madison, WI 53706, USA
e-mail: jek@wisc.edu

X. Liu
Chinese Academy of Sciences,
Institute of Earth Environment,
10 Fenghui South Road,
High-Tech Zone, Xi'an 710075,
People's Republic of China

1 Introduction

During the past 25 years, the response of regional monsoon systems to changes of insolation caused by orbital forcing has been studied using so-called equilibrium climate simulations. In these simulations, the climate is forced by repeated (identical) seasonal insolation regimes for particular times, such as 6,000, 9,000, or 125,000 years ago (Kutzbach 1981; Kutzbach and Otto-Bliesner 1982; Hewitt and Mitchell 1998, Montoya et al. 2000; Liu et al. 2003). These simulations have provided "snapshots" of the equilibrium climate for a prescribed seasonal insolation regime (a function of season of perihelion, axial tilt, and orbital eccentricity). Comparisons of these simulations with observations of paleomonsoons have provided strong confirmation of the role of orbital forcing in causing the large observed changes in monsoons. This modeling approach has been a logical first step toward exploring the full range of climate response to changing orbital forcing, given limitations of computer resources.

However, simulating only the equilibrium response to orbital forcing ignores possible lead/lag effects within the climate system that could be expected to occur as the orbital forcing changes progressively with time. For example the month of perihelion moves through the calendar year by about one month every 1,850 years following the 22,000-year precession cycle, and land and ocean may be expected to react differently to the seasonal timing of perihelion.

By analogy, the first three-dimensional climate model simulations were made for equilibrium January and July insolation extremes, and were therefore incapable of simulating the lagged response of sea-surface temperature (SST) to the seasonal insolation cycle owing to the ocean's considerable heat capacity and mixing depth. Some previous work using energy budget models (Short and Mengel 1986) or an accelerated three-dimensional atmospheric model coupled to a slab ocean (Jackson and Broccoli 2003) point toward interesting features of the climate's response to time-dependent orbital forcing. Tuenter et al. (2005) performed transient simulations with a coupled model of intermediate complexity to explore climate phase lags in response to precession and obliquity forcing from 280,000 to 150,000 years ago. Very recently, advances in computer speed have made it possible to simulate the continuous evolution of Holocene monsoons to time-dependent orbital forcing for the past 6,000 years (Liu et al. 2006). However, the response of tropical monsoons, and in particular, monsoon precipitation, to time-dependent orbital forcing spanning almost 300,000 years and many precession and tilt cycles has heretofore not been addressed with general circulation climate models, and is the topic of this paper (Sect. 3).

Along with advances in modeling capabilities, new observational studies are adding to our knowledge of the relationship between orbital forcing and monsoon response. While many studies have generally confirmed the close temporal linkage between orbitally-caused summer insolation maxima and monsoon maxima, others point toward significant lags of more than several thousand years. Some of these differences have recently been addressed by Ruddiman (2006) and Clemens and Prell (2007).

This paper uses a fast ocean–atmosphere climate model and accelerated orbital forcing (Sect. 2) to simulate the transient climatic response to orbital forcing changes over the past 280,000 years. We describe the simulated phase relationships between orbital forcing and monsoon related indices of land and ocean temperature, land/ocean temperature contrasts, land sea-level pressure, and precipitation (Sect. 3). The results suggest that the simulated timing of maximum monsoon response to orbital forcing is influenced both by the timing of ocean temperature response (which influences evaporation and landward moisture transport) and by land/ocean temperature contrast and lowered pressure over the continents (which influences the primary circulation response) (Sect. 3). We conclude with a brief comparison of these regional-scale monsoon simulations with a selective survey of paleomonsoon observations (Sect. 4).

2 Model approach and analysis techniques

To conduct a climate simulation covering 284,000 years, or about 12 precession cycles and seven tilt cycles, we use a very fast climate model and an accelerated orbital forcing scheme.

2.1 Model

We use a fully coupled global ocean–atmosphere model (FOAM). The atmospheric component of FOAM is a fully parallel version of the NCAR CCM2, in which the atmospheric physics representation is from CCM3 (Jacob 1997). The atmospheric model has a horizontal resolution of R15 (equivalent grid spacing of about 4° latitude by 7.5° longitude) and 18 vertical levels. The z-coordinate oceanic component of FOAM, the Ocean Model version 3 (OM3), is based upon the Geophysical Fluid Dynamics Laboratory Modular Ocean Model (GFDL MOM); it has a horizontal resolution of 1.4° latitude by 2.8° longitude and 24 vertical levels. FOAM runs efficiently on parallel computing systems (Jacob et al. 2001) and produces a steady long-term climate without using flux adjustment. As reviewed in Liu et al. 2003, FOAM simulates most major features of the observed tropical climate and in particular the major features of the summer monsoons in both northern and southern hemispheres. The response of these summer monsoons to orbital forcing as simulated by FOAM is similar to the response simulated by the higher resolution NCAR CSM (Liu et al. 2003).

2.2 Acceleration scheme

We accelerate the orbital forcing by a factor of 100, so that the actual length of our simulation, following spin-up, is 2,840 years. That is, at the end of each year of the simulation, we advance the orbital parameters (longitude of perihelion, axial tilt, and eccentricity; see Berger 1978) by 100 years. Given that the response time of the atmosphere-upper ocean system is of the order of a decade, or about 1,000 times faster than the shortest orbital cycle (precession), this acceleration is justified. Jackson and Broccoli (2003) gave similar

arguments for using an acceleration factor of 30 in a simulation of the past 165,000 years. We will restrict ourselves to analysis of the response of the upper ocean, and in particular the SST to this accelerated forcing, because the deeper ocean with its much longer response time cannot be expected to respond realistically to the accelerated forcing. Timmermann et al. (2007) simulated the global climate of the last 140,000 years using an acceleration factor of 100 in a fully coupled ocean-atmosphere model. Their analysis suggests a quasi-equilibrium response to the orbital forcing in the upper ocean. In another study using accelerated forcing in a fully coupled model, Lorenz and Lohmann (2004) found that acceleration factors of 10 and 100 produced similar results. The full range of insolation change over a half precession cycle ($\sim$10,000 years) is of order 50 W/m^2, and therefore the change in insolation forcing from year to year with the acceleration factor of 100 is generally less than 0.5 W/m^2 at all latitudes.

2.3 Spin-up

We started the integration using orbital forcing parameters for 284,000 years ago. The model was run for $\sim$200 actual years under the prescribed orbital forcing before commencing the accelerated simulation from 284,000 years ago to the present. For practical reasons, the simulation of these 2,840 years (actual years of the simulation) was divided into four segments averaging about 800 years each, with about 100 years of overlap in each segment. The overlapped segments were then combined using a weighted average.

2.4 Other boundary conditions

We address only the response of the model to orbitally-caused changes of insolation. Changes in atmospheric greenhouse gases, atmospheric dust loading, continental ice sheets, and sea-level are ignored in this initial study, but could be included in subsequent simulations.

2.5 Summer monsoon focus

We focus on the respective summer seasons of each hemisphere (J, JJA, and JJAS in the north; D, DJF, DJFM in the south). We have summarized the results using the modern calendar which does not take into account the changes in length of months and seasons that occur with the changing season of perihelion, the so-called "calendar effect" (Kutzbach and Gallimore 1988; Joussaume and Braconnot 1997).

2.6 Analysis techniques

We examine time series of the primary monsoon indicators and use cross-spectral analysis (Hannan 1970) between early summer insolation and various monsoonal indicators to derive coherence and phase lead/lag relationships between the external orbital forcing reference point and the internal climate response. The simulations of climate variables in the six monsoon regions, and the tropics/subtropics in general, exhibit a strong response to orbital forcing associated with the precession cycle, a period of about 22,000 years. In this paper, we focus exclusively on the precession cycle.

3 Results

3.1 Land temperature and ocean temperature

We will focus our analysis on monsoon precipitation, but we first examine the response of land temperature (20°–40°N, and 20°–40°S) and SST in several ocean regions (Fig. 1) to the changing insolation. At the seasonal cycle, the maxima in land and ocean temperature lag the maxima in insolation forcing due to the thermal inertia of land and ocean. This lag may be of order 1 month over land and 2 months over ocean. For example, northern land temperature maxima may occur in late July, about a month after the June 21st insolation maxima, and northern ocean temperature maxima may occur in August, or later, about 2 months after insolation maxima. At the precession cycle, we find (described below) that land and ocean temperature also exhibit a lagged response to changes in orbital forcing. For example, when perihelion occurs in April, we find that the northern tropical SST exhibits its largest response in June. And, about one-twelfth of a precession cycle later (about 1,850 years later), when perihelion has advanced to May, we find that the northern tropical SST exhibits maximum response in July. This lagged response will be described in more detail below.

We will use JJA and DJF averages to express the conventional summer conditions for northern and southern hemispheres. In relating orbital forcing maxima for a particular month (April, May, June, for example) to the monsoon response, we will sometimes refer to the phase lags with respect to the mid-month of the conventional three-month summer average, i.e., July or January.

In addition to describing the lagged response of monsoon indices to orbital forcing, it is also convenient to express all phases relative to a fixed orbital reference point. We will use northern (southern) hemisphere June (December) insolation as the basis for summarizing phase relations. The insolation at the summer solstice (June 21 or

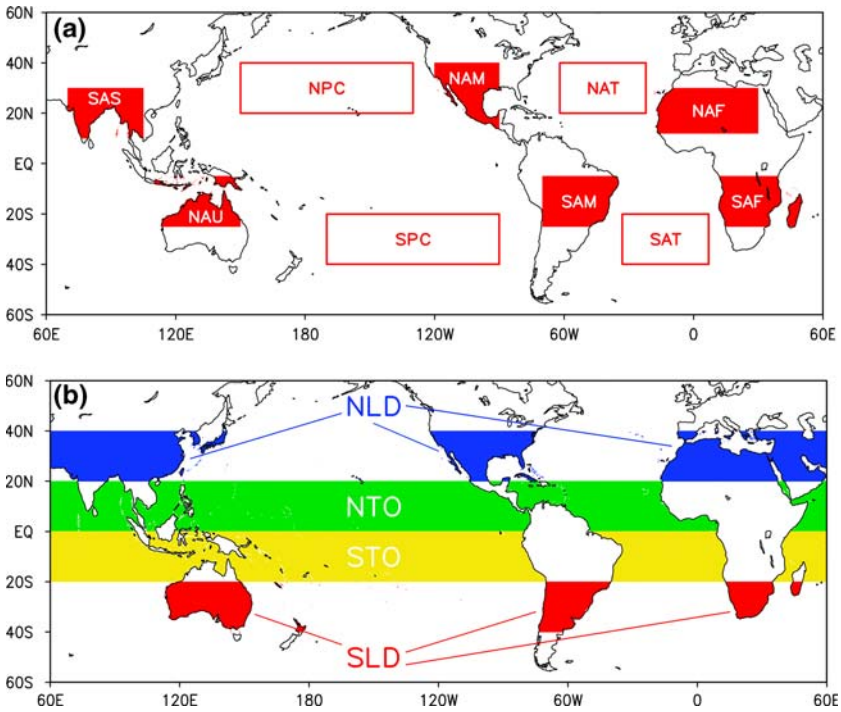

Fig. 1 Locations of area-average domains for six monsoon regions and several land and ocean regions used in this study. **a** The six monsoon regions include South Asia (SAS), north Australia (NAU), North America (NAM), South America (SAM), North Africa (NAF) and South Africa (SAF); the four mid-latitude ocean regions include the North Pacific Ocean (NPC), South Pacific Ocean (SPC), North Atlantic Ocean (NAT) and South Atlantic Ocean (SAT). **b** The broad regions representing climates of northern (southern) land, NLD (SLD), and northern (southern) tropical ocean SSTs, NTO (STO). See text for details

December 21) is frequently chosen as a baseline reference point and our use of June or December insolation is a close approximation to this reference.

The maxima and minima in the simulated time series of JJA (DJF) land temperature follow closely the maxima and minima in June (December) insolation for the three northern (southern) regions (Fig. 2). The amplitude of the land temperature response is larger in the northern hemisphere (about 6 K) than in the southern hemisphere (about 4 K), a result expected based upon the larger size of the northern continents. The physical lag between forcing and response due to thermal inertia of the land is about 30° at the precession period, with June (December) insolation correlating highest with July (January) land temperature, which is the mid-point of JJA (DJF). In Fig. 2, this phase lag manifests itself as an almost in phase relation between June (December) orbital forcing and JJA (DJF) land temperature response. The phase relations relative to the June (December) reference insolation are summarized in Fig. 3 and Table 1.

The maxima in the time series of JJA (DJF) SST for the northern (southern) tropical oceanic regions, NTO and STO, exhibit a phase lag between forcing and response due to thermal inertia of the oceans of about 60° at the precession period (Fig. 2, Table 1). In other words, the maxima in July (January) SSTs, the mid-points of the JJA (DJF) SST averages, correlate closely with the May (November) insolation maxima. Alternatively, comparing the time series of JJA (DJF) NTO (STO) SST to the reference June (December) insolation time series (Fig. 2), the SST reach maxima ahead of the reference insolation. The phases for both tropical and mid-latitude ocean SST, relative to the reference insolation, are summarized in Fig. 3 and Table 1.

In summary, using the northern hemisphere as an example, we found from cross-spectral analysis that June SST has maximum coherence and ~0 phase angle with April insolation, i.e., June SST has maximum positive correlation with April insolation. Therefore June SST lags April insolation by about 60° at the precession cycle. In a corresponding fashion, July SST (the mid-point of JJA) lags May insolation by about 60° and August SST lags June insolation by 60°. It follows that when SST is combined to form the conventional summer average (JJA) it exhibits a phase lag of 60° with respect to May insolation. Alternatively, from the perspective of a June insolation reference point, JJA SST leads the June insolation reference by 30°. The numbers in this example are rounded for illustrative purposes. The phase lag of JJA SST relative to late spring/early summer insolation forcing at the precession period is consistent with the results of climate model simulations reported by Jackson and Broccoli (2003) and Tuenter et al. (2005) for the relation of sub-tropical or mid-latitude monthly surface air temperature maxima to the month of perihelion. Short and Mengel (1986) also obtained similar results using an energy balance climate model. However we compared the SSTs of a specific month, or months, to June (December) insolation whereas Short and Mengel found the phase lag of the maximum SST anomaly (regardless of month) relative to the June (December) insolation.

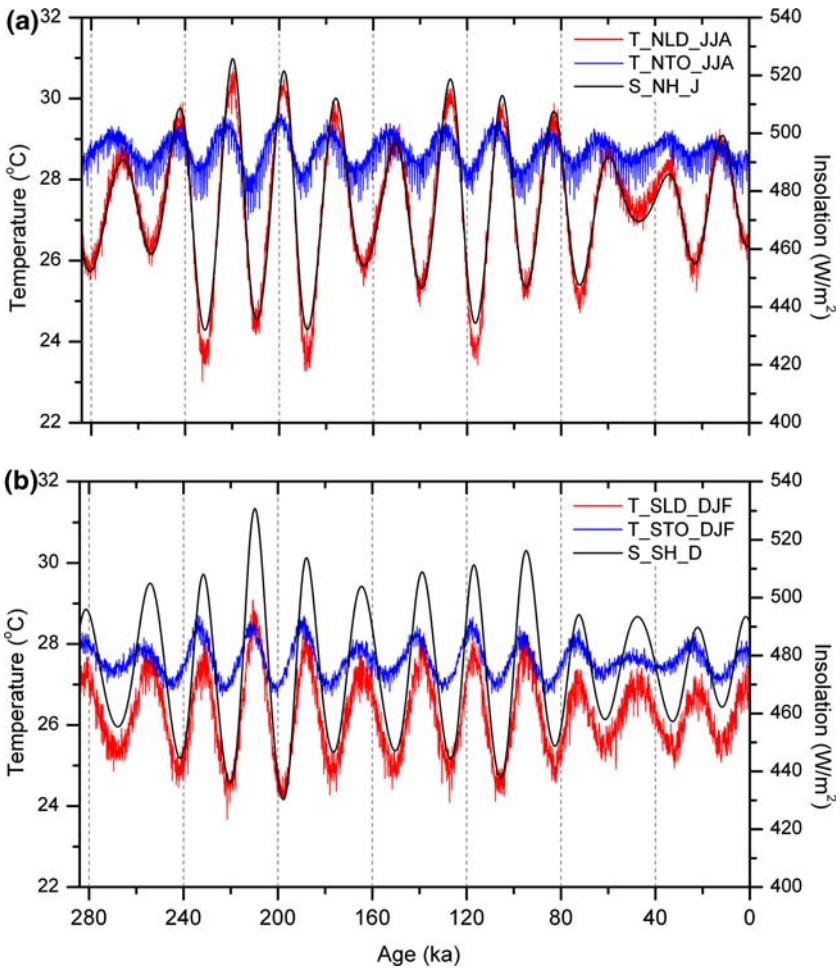

Fig. 2 **a** Time series of NH June insolation (S_NH_J) and JJA surface air temperatures averaged for NH mid-latitude (20°–40°N) land (T_NLD_JJA) and NH tropical (0°–20°N) ocean (T_NTO_JJA). **b** Time series of SH December insolation (S_SH_D) and DJF surface air temperatures averaged for SH mid-latitude (20°–40°S) land (T_SLD_DJF) and SH tropical (0°–20°S) ocean (T_STO_DJF)

3.2 Summer monsoon precipitation

We have investigated the simulated response of summer monsoon precipitation to orbital forcing in six regions: North Africa, South Asia, and North America in the northern hemisphere, and South Africa, north Australia, and South America in the southern hemisphere (Fig. 1). These same six regional monsoons were examined in a previous study of changes in monsoons during the Holocene (Liu et al. 2003).

The maxima and minima in the time series of JJA (DJF) precipitation are approximately in phase with the corresponding June (December) insolation time series (Fig. 4). The amplitude of the response varies from region to region. In percentage terms, the North African, South Asian, and north Australian monsoons show the largest range of variation (±40% or more), while the North American, South African, and South American monsoons show the smallest range (about ±15% or less). This relative sensitivity of regional monsoons to orbital forcing is largely consistent with results from equilibrium (snapshot) simulations at particular times within the Holocene (Liu et al. 2003)

The average phase of the six monsoon precipitation time series (Table 2) is ~0° relative to the appropriate June or December reference insolation, which implies an average lag between insolation forcing and JJA or DJF precipitation response of about 30° at the precession period. In the northern hemisphere, the South Asian monsoon precipitation (JJA) responds more to late spring/early summer forcing while the North African monsoon (JJA) is almost exactly in phase with the June insolation reference (Fig. 5, Table 2). Using a climate model of intermediate complexity, Tuenter et al. (2005) obtain a very similar lagged response of summer monsoon precipitation to summer precession forcing. For a large sector representing both North Africa and South Asia, they report monthly phase angles for precipitation that, when combined for JJA, are almost exactly in phase with the June insolation reference. The physical interpretations of these phase relationships are addressed in Sect. 3.3.

In the southern hemisphere, the South African monsoon precipitation (DJF) is almost exactly in phase with the December insolation reference while the South American and north Australia monsoons exhibit small phase lags of

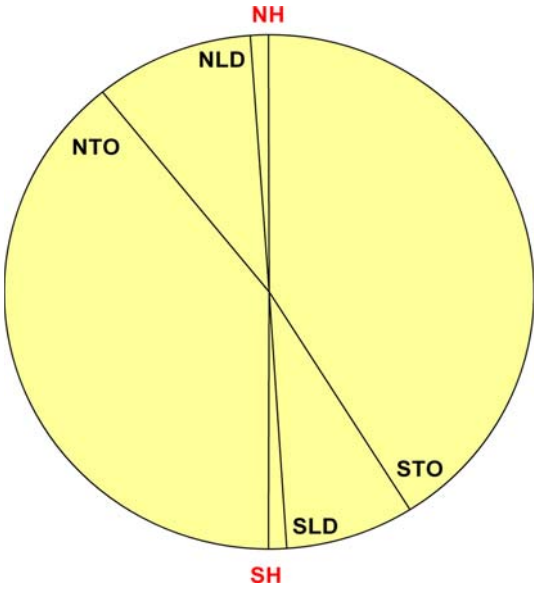

Fig. 3 Phase relations of JJA (DJF) surface temperature for northern (southern) land, NLD (SLD), and for northern (southern) tropical ocean, NTO (STO), relative to northern (southern) hemisphere June (December) reference insolation, NH (SH). The land surface temperatures are for 20°–40°N (20°–40°S); the ocean surface temperatures are for 0°–20°N (0°–20°S) (Fig. 1b). The phase wheel is for the precession cycle, 22,000 years, with phase leads (lags) shown counterclockwise (clockwise) relative to the northern and southern hemisphere insolation reference. Note that the reference insolation is June (December) whereas the simulation responses are JJA (DJF). Thus an "in phase" alignment between the reference insolation and the climate response implies a 30° phase lag of the response relative to the forcing. Physical leads/lags are discussed in the text

Table 1 Phases (degrees and years) at the precession band obtained from cross-spectral analyses: (top) between NH June insolation and JJA surface temperatures for NH mid-latitude land and oceans, and tropical oceans; (bottom) between SH December insolation and DJF surface temperatures for SH mid-latitude land and oceans, and tropical oceans.

Region		Phase: degrees	Phase: years
N. Mid. land	NLD	4	250
N. Pacific	NPC	36	2,200
N. Atlantic	NAT	31	1,900
N. Tropical	NTO	39	2,400
S. Mid. land	SLD	4	250
S. Pacific	SPC	45	2,750
S. Atlantic	SAT	45	2,750
S. Tropical	STO	32	1,950

A positive (negative) phase means the climate variable leads (lags) the reference insolation (see text for discussion of physical leads/lag relations). Coherence at the precession band exceeds 0.97 in all cases. Phases are rounded to the nearest degree and nearest 50 years. A precession period of 22,000 years is used to convert degrees to years

15 and 19° (900 and 1,150 years), respectively (Fig. 5, Table 2). Thus on average the southern monsoons exhibit a somewhat larger phase lag than the northern monsoons relative to the respective summertime orbital forcing.

In summary, there is an average phase lag of 30° between June (December) insolation and the mid-month of the summer precipitation, July for JJA and January for DJF. However, there is some spread about this average result, with South Asian monsoon precipitation responding to late spring/early summer forcing and north Australian monsoon precipitation responding to mid-summer forcing (Table 2). The times series of JJAS (DJFM) precipitation for the northern (southern) regions exhibit, on average, about an 11° phase lag relative to the reference June or December insolation (Table 2), which implies an average 40° phase lag between June (December) insolation forcing and the mid-point of the 4-month summer precipitation. This difference in lag depending on the choice of 3- or 4-month summer averages can be a factor in interpretation of proxy observations of monsoons, where the length of the appropriate seasonal monsoon average is often unknown (Sect. 4).

3.3 Monsoon dynamics perspective

We reported in Section 3.1 that land (ocean) temperature maxima where phase-lagged relative to insolation by about 30 (60)°, and we also associated these responses with the June (December) insolation reference (Tables 1, 2). In this section, we compare various land and ocean thermal responses to the monsoon precipitation responses and show that the precipitation indices exhibit phase lags intermediate between land and ocean indices.

Fundamental ideas about monsoon processes (Webster 1987) invoke the roles of both land/ocean thermal contrasts (thermal/dynamic processes) and the roles of water transport from oceans to land via evaporation and horizontal advection (hydrologic/dynamic processes). One might expect that monsoon precipitation would exhibit a phase relationship relative to insolation that lies somewhere within the limits of the phase extremes exhibited by the thermal/dynamic and hydrologic/dynamic processes, depending upon their relative importance.

To explore this possibility, we constructed time series of mid-latitude (20°–40°N or S) land/ocean temperature contrasts, and land sea-level pressure, for JJA (DJF) (Table 3). The land/ocean temperature contrast for JJA (DJF) for the northern (southern) hemisphere lags the June (December) insolation reference by 11° (26°). The minimum sea-level pressure over land for JJA (DJF) for the northern (southern) hemisphere lags the June (December)

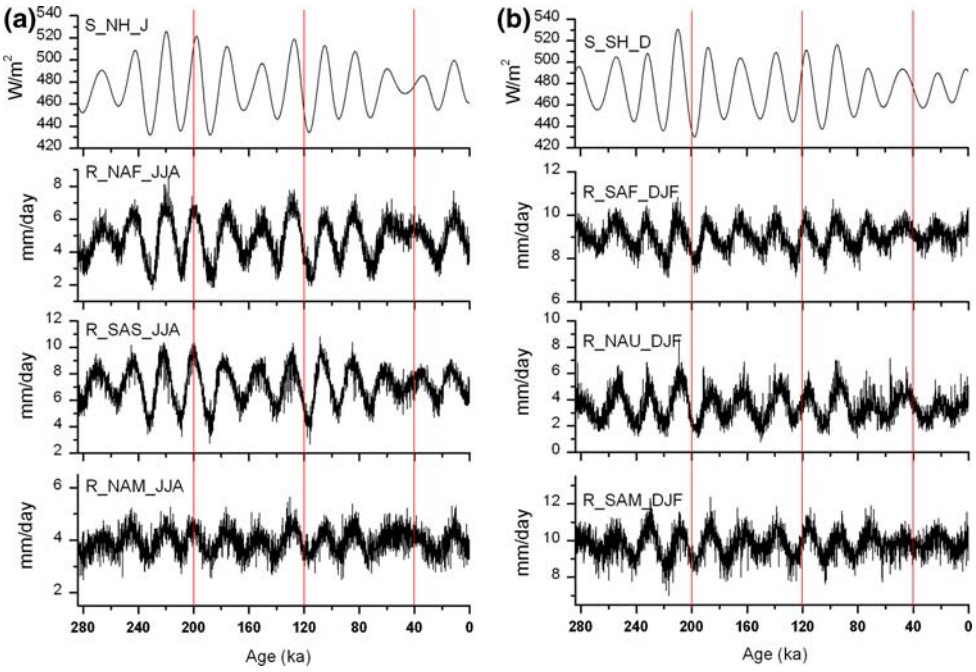

Fig. 4 **a** Time series of NH June insolation (S_NH_J) and JJA precipitation rate averaged for North Africa (R_NAF_JJA), South Asia (R_SAS_JJA) and North America (R_NAM_JJA). **b** Time series of SH December insolation (S_SH_D) and DJF precipitation rate averaged for South Africa (R_SAF_DJF), north Australia (R_NAU_DJF) and South America (R_SAM_DJF)

insolation reference by amounts almost identical to those for the land/ocean temperature contrasts: 10° (28°). Energy-balance models with a slab ocean yield similar indications that maximum land/ocean temperature contrasts lag summer insolation maxima (Short and Mengel 1986; Guangshan Chen, not shown).

Comparing the phases of these indices of land/ocean thermal contrast and land sea-level pressure (thermal/dynamic processes, "t") and the aforementioned tropical SST indices NTO and STO (hydrologic/dynamic processes, "h") to the phases of the precipitation indices,

Table 2 Phases (degrees and years) at the precession band obtained from cross-spectral analyses: (top) between NH June insolation and JJA (JJAS) precipitation for three NH monsoon regions; (bottom) between SH December insolation and DJF (DJFM) precipitation for three SH monsoon regions

Region		Phase: degrees	Phase: years
North Africa	NAF	–1 (–10)	–50 (–600)
South Asia	SAS	23 (14)	1,400 (850)
North America	NAM	14 (13)	850 (800)
South Africa	SAF	3 (–16)	200 (–1,000)
North Australia	NAU	–19 (–31)	–1,150 (–1,900)
South America	SAM	–15 (–36)	–900 (–2,200)

A positive (negative) phase means the climate variable leads (lags) the reference insolation (see text for discussion of physical lead/lag relations). Coherence at the precession band exceeds 0.97 in all cases. Phases are rounded to the nearest degree and nearest 50 years. A precession period of 22,000 years is used to convert degrees to years

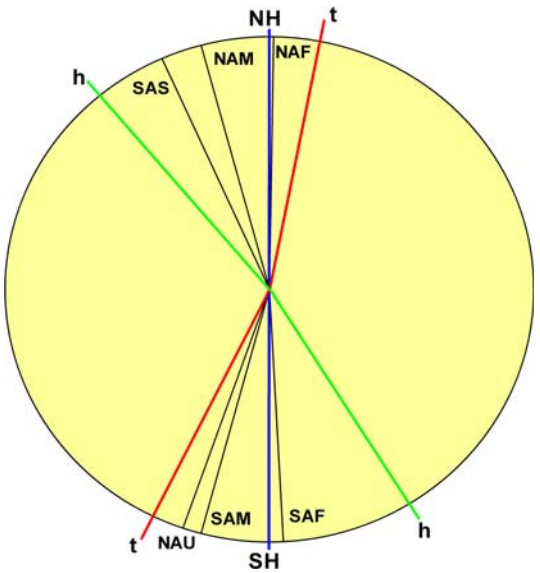

Fig. 5 Phase relations of JJA (DJF) precipitation rate for three northern (southern) monsoon regions, NAF, SAS, NAM (SAF, NAU, SAM), relative to northern (southern) hemisphere June (December) reference insolation, NH (SH). The monsoon regions are as labeled and described in Fig. 1. The phase wheel is for the precession cycle, 22,000 years, with phase leads (lags) shown counterclockwise (clockwise) relative to the northern and southern hemisphere insolation reference. The *lines* labeled "h" and "t" on the phase circle indicate the phases of the hydrologic (h) process indices NTO (STO) and the thermal (t) indices relative to the June (northern) and December (southern) insolation reference. Note that the reference insolation is June (December) whereas the simulation responses are JJA (DJF). Thus an "in phase" alignment between the reference insolation and the climate response implies a 30° phase lag of the response relative to the forcing. Physical leads/lags are discussed in the text

Table 3 Phases (degrees and years) at the precession band obtained from cross-spectral analyses: (top) between NH June insolation and JJA mid-latitude (20°–40°N) land/ocean surface temperature difference, and JJA mid-latitude land sea-level pressure minimum; (bottom) between SH December insolation and DJF mid-latitude (20°–40°S) land/ocean surface temperature difference, and DJF mid-latitude land sea-level pressure minimum

Region	Phase: degrees	Phase: years
N. Land/ocean temperature difference	–11	–650
N. Land sea-level pressure minimum	–10	–600
S. Land/ocean temperature difference	–26	–1,600
S. Land sea-level pressure minimum	–28	–1,700

A positive (negative) phase means the climate variable leads (lags) the reference insolation (see text for discussion of physical lead/lag relations). Coherence at the precession band exceeds 0.97 in all cases. Phases are rounded to the nearest degree and nearest 50 years. A precession period of 22,000 years is used to convert degrees to years

we find that all six precipitation indices have phases that lie within the limits of the broad scale hydrologic/thermal process indices (Fig. 5).

A temporal view of these phase relationships among the thermal and hydrologic process indices and the monsoon precipitation indices is obtained by compositing the results from the 284,000-year time series relative to the maxima in the June insolation reference for ten precession cycles. The composite results for the northern hemisphere are plotted for leads/lags of ±15,000 years relative to the June insolation reference at 0 years. The maximum JJA land temperature, maximum JJA land/ocean temperature contrast, and minimum JJA land sea-level pressure are all approximately in phase with the June insolation reference, indicating again the approximate 30° phase lag (about 1,850 years) of the mid-month of these 3-month averaged variables relative to June insolation forcing. The maximum JJA SST averaged from 0° to 20°N (NTO) occurs before the maximum June insolation reference by about 2000 years, indicating the larger physical lag of SST in response to insolation forcing. The times of maximum JJA precipitation in the three northern monsoon regions fall between these times of maximum land and ocean temperature (Fig. 6).

In summary, we find that the summer monsoon precipitation indices exhibit phases that fall within the phase limits defined by our admittedly crude indices of hydrologic/dynamic and thermal/dynamic processes. It is beyond the scope of this paper to examine in more detail the results for each region. Each of the six regions has unique geographic, topographic, and oceanic features that would require a more refined analysis.

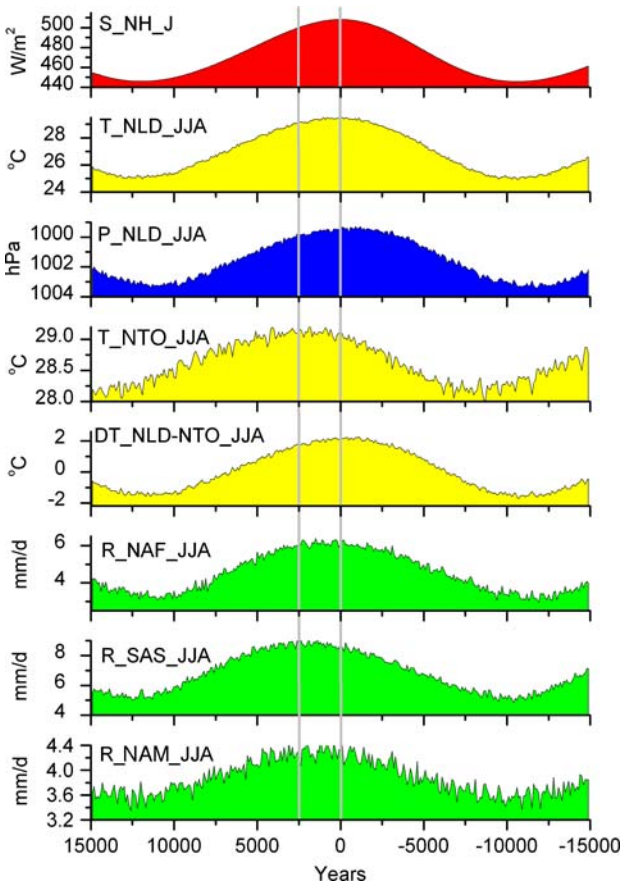

Fig. 6 Composite analyses of JJA surface air temperature (T_NLD_JJA) and sea level pressure (P_NLD_JJA) over northern mid-latitude land (20°–40°N), surface air temperature (T_NTO_JJA) over global northern tropical ocean (0°–20°N), JJA land/ocean temperature difference anomaly (DT_NLD-NTO_JJA) and JJA precipitation rate for North Africa (R_NAF_JJA), South Asia (R_SAS_JJA) and North America (R_NAM_JJA) with respect to NH June insolation reference (S_NH_J). The positive (negative) years in the horizontal axis indicate that the climatic element in JJA leads (lags) the June insolation reference. The composite analyses are based upon ten precession cycles from time series such as those shown in Figs. 2 and 4. Note that the reference insolation is June whereas the simulation responses are JJA. Thus an "in phase" alignment between the reference insolation and the climate response implies a 30° phase lag of the response relative to the forcing. Physical leads/lags are discussed in the text

4 Comparison with observations

Observational studies have been used to explore the lead/lag relations of internal climate system components to changes in external forcing. Perhaps the most comprehensive time series analysis of the observed climate system behavior, relative to orbital forcing, was the series of papers by the SPECMAP group which documented the phase relationships between insolation and glacial/interglacial climates as represented by ice volume, various ocean SST or sea-ice indicators, and ice core records (Imbrie et al. 1993). These kinds of studies have been less

commonly used for analysis of paleomonsoons and orbital forcing, due in part to shorter records. However, Clemens and Prell (2003) used cross-spectral analysis of a long multi-proxy record of the Arabian Sea monsoon to infer lead/lag relationships with orbital forcing.

A detailed comparison of our simulations with observations is not appropriate at this time for several reasons: (1) our simulation is forced only by orbital changes, whereas observations record the response to glacial cycles, including greenhouse gas changes, as well as orbital cycles; (2) observations have a variety of record lengths and dating uncertainties; and (3) observations may reflect monsoon changes not well characterized by precipitation, or by a particular period of precipitation.

The first point is important because previous modeling studies have indicated that monsoons respond both to orbital and glacial boundary condition forcing (Prell and Kutzbach 1992). The second point relates to potential errors in cross-spectral analysis that can result from short records or records with relatively poor chronologic control. The third point is illustrated by noting that phase relationships vary depending upon the averaging period for the summer monsoon. In Sect. 3, we focused on the conventional 3-month (JJA or DJF) average. However, a 4-month average (JJAS or DJFM) represents a better estimate of the total summer monsoon precipitation based upon the FOAM model climatology. As expected, if one extends the summer monsoon period by 1 month (September or March), the corresponding phases relative to early summer insolation show increased lag (Table 2). Therefore if proxy monsoon indicators reflect the overall strength of the monsoon, then the phase information for the 4-month averages would be more relevant for comparison of data with models. Differences in phase might also result from choices of different variables (winds, upwelling, cloudiness) or different averaging periods. Braconnot and Marti (2003) used modeling studies to show that changes in the seasonal timing of maximum insolation forcing anomalies can influence the timing and length of the monsoon season as well as the strength of the monsoon, and that these factors may also help account for observed regional differences in phase relations. Tuenter et al. (2005) report that the combined North Africa/South Asia summer monsoon precipitation increases in September and May (as well as JJA) when perihelion occurs in northern summer, and that this leads to an overall lengthening of the summer monsoon season at those times. It is also true that different regions may have different absolute or relative sensitivities to orbital forcing. For example, in this study we find that the relative sensitivity of monsoon precipitation to insolation forcing is largest for NAF, SAS, and NAU (Table 4).

With these caveats in mind, we will review selected papers describing long monsoon records from four of the six regions (North Africa, South Asia, north Australia, and South America). We are not aware of long records (longer than 100,000 years) for the North American or South African monsoons. Our selective review is far from complete. Where possible, we mention two kinds of papers for each region: papers that show approximate in-phase relationships of the summer monsoon response to summertime orbital forcing, as found in this modeling study, and papers that also emphasize a strong influence of glacial boundary condition forcing or other factors that cause large phase lags of the monsoon relative to summertime orbital forcing, i.e., lags exceeding significantly those found in our modeling study. The purpose of including both types of results is to illustrate that much work remains to fully understand the causes of the observed climatic history of monsoons.

Table 4 Mean value, minima and maxima [absolute and (percent)], and standard deviations for insolation (S, in W/m^2) and monsoon precipitation (R, in mm/day)

Variable	Mean	Minima	Maxima	Standard deviation
S, NH	475	433 (–9%)	525 (11%)	22
R, NAF	4.8	2.3 (–52%)	6.9 (44%)	1.1
R, SAS	7.1	4.2 (–41%)	9.6 (35%)	1.3
R, NAM	3.9	3.3 (–15%)	4.6 (18%)	0.3
S, SH	476	431 (–9%)	530 (11%)	21
R, SAF	9.0	7.7 (–14%)	10.0 (11%)	0.5
R, NAU	3.5	1.8 (–49%)	5.8 (66%)	0.9
R, SAM	9.8	8.5 (–13%)	11.0 (12%)	0.5

Minima and maxima and standard deviations were derived after smoothing the original time series with a 2000-year running mean filter. Monsoon regions are identified in Fig. 1. Northern hemisphere variables are for June (insolation) and JJA (precipitation). Southern hemisphere variables are for December (insolation) and DJF (precipitation)

4.1 North Africa

Rossignol-Strick (1983) used a 460,000-year record of East Mediterranean sapropels to infer an approximate in-phase relationship between the African monsoon and an insolation index weighted towards northern summer. Pokras and Mix (1987) used a 260,000-year record of freshwater diatoms deposited in Atlantic ocean sediments to infer a close relationship between wet/dry cycles of the African monsoon and the absence/presence of freshwater diatoms transported westward by winds from lake beds in tropical Africa (their diatom index led the insolation index by about 35°, a result they explained as either a sensitivity to late spring/early summer perihelion or a nonlinear effect due to maximum deflation occurring early in the dry phase of the precession cycle). In contrast to these findings of relatively

in-phase response of the monsoon to orbital forcing, other studies have inferred a mix of orbital forcing and glacial forcing influences on the North African monsoon (deMenocal 2004). Zabel et al. (2003) used a 240,000-year record of fluvial deposits from the Niger delta to infer that the African monsoon responded to orbital forcing at the precession period but with a phase lag of about 65° (4,000 years) and to a precessional component of glacial forcing with a phase lag of about 180° (i.e., strongest monsoons with weakest glacial forcing).

4.2 South Asia/East Asia

Yuan et al. (2004) used a 160,000-year record of isotopic ratios from stalagmites in two caves in southern China to infer an in-phase relationship between the Asian monsoon and JJA insolation, particularly for the largest insolation excursions during the last interglacial (they note that the abruptness of onset or termination may be related to higher latitude forcing). An et al. (1991) used a 130,000-year record of magnetic susceptibility from loess deposits in central China to infer an approximate in-phase relation between monsoon precipitation and summertime insolation maxima at the precession time scale although several of the precession-related peaks are relatively small. Sun and Huang (2006) found in-phase relationships for the largest precession peaks and also half-precession cycles. These land-based estimates of the Asian monsoon are from locations near or outside the margin of the area average we used for South Asia, but the model results would not have been greatly different had we chosen a slightly larger area. In contrast to these results that infer approximate in-phase response of monsoons to orbital forcing, others find relatively large phase lags and links to glacial boundary condition forcing or other factors. For example, Clemens and Prell (2003) used a 350,000-year multi-proxy record from the northern Arabian Sea (also outside the box of our land precipitation index) to infer that monsoon-induced upwelling lagged 21 June perihelion by about 120° (7,000–8,000 years) at the precession period owing to the combined influence of northern hemisphere summer insolation, northern glacial forcing (glacial minima lag insolation maxima) and southern hemisphere latent heat input. A large phase lag between precession forcing and Arabian Sea upwelling indictors has been linked in part to increased late summer insolation (Reichart et al. 1998). Other studies also report large phase lags for the East Asian summer monsoons, relative to orbital forcing: Morley and Heusser (1997), Chen et al. (2003) and Wang et al. (2005). While the South Asian phase results simulated in this study do not compare well with these late Pleistocene data (noting again that our model did not include glacial forcing), geological data from the late Pliocene (prior to significant northern hemisphere glaciation) do compare well with the phase results found in our simulations (Clemens and Prell, personal communication).

4.3 North Australia

Bowler et al. (2001) used a 300,000-year record of lake levels in northern Australia to infer a likely role of orbital forcing in periodic enhancement of the north Australia monsoon, but the dating uncertainties of these records complicate the assessment of the relative importance of northern hemisphere or southern hemisphere orbital forcing. Magee et al. (2004) used 150,000-year records of lake levels in south-central Australia to infer that insolation minima during northern hemisphere winter are more important than insolation maxima in southern hemisphere summer in causing some of the observed lake level changes. This would imply a 180° phase lag of the Australian monsoon maxima with respect to southern hemisphere insolation maxima; however, they note that dating uncertainties remain. The model results reported in this paper, and others (Liu et al. 2003; Wyrwoll and Valdes 2003), indicate instead the approximate in-phase response of the Australian summer monsoon to southern summer insolation forcing. The exception to this in-phase response in model results is that a strong oceanic feedback mechanism along the western coastal region of Australia does produce the out-of-phase response that counters the direct insolation response (Liu et al. 2003).

4.4 South America

Cruz et al. (2005) used 116,000-year records of isotopes from stalagmites in caves in southern Brazil to infer an in-phase response of the South American summer monsoon to February insolation maxima (although noting that some glacial boundary forcing from the northern hemisphere may also be evident).

4.5 Discussion

While many observational studies in North Africa, Asia, and South America strongly support the simulated close relationship between summertime orbital forcing and summer monsoon response, there are some that show differences. For example, the monsoon proxies from speleothem records in China (Brazil) present comparisons of the observations with JJA (February) insolation anomalies, whereas the model results would suggest best

correlations with May (December–January) insolation anomalies. If we had made our comparisons with 4-month instead of 3-month precipitation averages (Table 2), the best model correlations would have shifted by almost one-half month: to May–June (January). This change in averaging interval would reduce but not eliminate the differences between the observations and the simulations. Errors in dating could also explain some model/observation differences. A shift of 1 month in the insolation time series (for example, June vs. July) corresponds to a shift of about 1,850 years in the chronology of the proxy, a difference that is small compared to the absolute dating of at least some of the records mentioned earlier in this section. Note also that the simulated results represent rather broad area averages and are therefore not point specific, as are some proxies. A number of observational studies based on marine sediment records, including some for North Africa and South and East Asia, find that glacial boundary conditions or other factors can be responsible for much larger phase lags between orbital forcing and monsoon response. In contrast to the growing number of long observational records of monsoons from North Africa, Asia, South America and northern Australia, we are not aware of long records (more than 100,000 years) of monsoon precipitation for North America or South Africa.

Differences in phase response between models and observations, and among models, may also stem from biases in climate models. The simulated phase response of climate to insolation forcing could be strongly dependent on the thermal inertia of the model's upper ocean and land. Different models might simulate different phase relationships, although our results regarding land and ocean temperature lags, and precipitation lags, are very similar to those found using a different model (Tuenter et al. 2005). Also, models could differ in the relative importance of land processes and ocean processes in determining the phases of monsoon precipitation relative to insolation forcing. For example, if the model used here had placed most weight on the influence of land temperature, land surface pressure, and land–ocean temperature contrast for setting the phase of monsoon precipitation (compared to the influence of SST), then our modeled precipitation phases might have been more consistent, relative to the timing of insolation forcing, with some of the cited land-based observations and with some previous model studies. Indeed, in some of our earlier studies with atmosphere-only models we used July insolation and July SSTs as upper and lower boundary condition forcing based upon the hypothesis that July insolation anomalies would have maximum effect on monsoon precipitation given the generally warmer conditions of July and the expectation that this warmth, through temperature-dependent water vapor feedback, might produce the maximum precipitation response to orbital forcing (Kutzbach and Otto-Bliesner 1982). While our simulation results using accelerated forcing suggest that the maximum northern monsoon response might be associated with June forcing rather than July forcing, we have given a number of reasons (above) why this result is preliminary. There is a need to evaluate the relative importance of various internal model processes for setting the phase of precipitation for individual regional monsoons with respect to insolation.

Our analysis has focused exclusively on the response of monsoons to the precession cycle (although the insolation forcing included changes in tilt). We chose this emphasis because the monsoon response to precessional forcing dominates our simulation and that of Tuenter et al. (2005). Most observations show the strongest monsoonal response to precession forcing, although some studies also report a strong response to obliquity forcing (for example, Clemens and Prell 2003).

5 Conclusions

An acceleration of orbital forcing by a factor of 100 allowed us to simulate a 280,000-year record of the response of both northern and southern hemisphere summer monsoons to orbital forcing in a fully coupled general circulation model. We find a strong and positive response of northern (southern) monsoon precipitation to northern (southern) summer insolation forcing. There is a lag between the orbital forcing and monsoon response. On average, July (January) precipitation maxima and JJA (DJF) precipitation maxima have high coherence and are approximately in phase with June (December) insolation maxima, implying an average lag between forcing and response of about 30° of phase at the precession period. The average lag increases to over 40° for 4-month precipitation averages, JJAS (DJFM). The phase varies somewhat from region to region, with the south Asian monsoon responding to late spring/early summer forcing and the north Australian monsoon responding to mid-summer forcing. The average JJA (DJF) land temperature maxima also lag the June orbital forcing maxima by about 30° of phase, whereas ocean temperature maxima exhibit a lag of about 60° of phase at the precession period.

The controls on monsoon precipitation are both thermal/dynamic (land/ocean temperature contrast, land sea-level pressure minima) and hydrologic/dynamic (relating to SST, evaporation from the ocean, and landward transport of water vapor). Using generalized measures of these controlling processes, we find that the summer monsoon precipitation indices for the six regions all fall within the phase limits of the process indices for the respective hemispheres.

Selected observational studies from four of the six monsoon regions also report approximate in-phase relations of summer monsoon proxies to summer insolation. However, some observational studies find substantial phase lags of summer monsoon proxies relative to summer insolation and a strong component of forcing associated with changing glacial-age boundary conditions or other factors. An important next step will be to include glacial-age boundary condition forcing in long, transient paleoclimate simulations, along with orbital forcing.

Acknowledgments The simulations were made at the NSF-sponsored computing facility of the National Center for Atmospheric Research (NCAR), Boulder, Co. This work was jointly supported by NSF grants to the University of Wisconsin-Madison (OCE-0352362), China's'973' Program (2004CB720208), and NSFC (40472086). We thank the reviewers. Their comments and suggestions improved the paper. This is Center for Climatic Research publication number 943.

References

An Z, Kukla GJ, Porter SC, Xiao J (1991) Magnetic susceptibility evidence of the monsoon variation on the Loess Plateau of Central China during the last 130,000 years. Quaternary Res 36:29–36

Berger AL (1978) Long-term variations in daily insolation and quaternary climate changes. J Atmos Sci 35:2362–2367

Bowler JM, Wywroll K-H, Lu Y (2001) Variation of the northwest Australian summer monsoon over the last 300,000 years: The paleoecological record of the Gregory (Mulan) Lakes system. Quat Int 83–85:63–80

Braconnot P, Marti O (2003) Impact of precession on monsoon characteristics from coupled ocean atmosphere experiments: changes in Indian monsoon and Indian ocean climatology. Mar Geol 201:23–34

Chen M-T, Shiau L-J, Yu P-S, Chiu T-C, Chen Y-G, Wei K-Y (2003) 500000-year records of carbonate, organic carbon, and foraminiferal sea-surface temperature from the southeastern south China Sea. Palaeogeogr Palaeoclimatol Paleaoecol 197:113–131

Clemens SC, Prell WL (2003) A 350,000 year summer monsoon multi-proxy stack from the Owen Ridge, Northern Arabian Sea. Mar Geol 201:35–51

Clemens SC, Prell WL (2007) The timing of orbital-scale Indian monsoon changes. Quaternary Sci Rev 26:275–278

Cruz FW Jr, Burns SJ, Karmann I, Sharp WD, Vuille M, Cardoso AO, Ferrari JA, Silva Dias PL, Viana O Jr (2005) Insolation-driven changes in atmospheric circulation over the past 116,000 years in subtropical Brazil. Nature 434:63–66

deMenocal PB (2004) African climate change and faunal evolution during the Pliocene–Pleistocene. Earth Planet Sci Lett 220:3–24

Hannan EJ (1970) Multiple time series. Wiley, New York, p 536

Hewitt CD, Mitchell JFB (1998) A fully coupled general circulation model simulation of the climate of the mid-Holocene. GRL 25:361–364

Imbrie J, Berger A, Boyle EA, Clemens SC, Duffy A, Howard WR, Kukla G, Kutzbach J, Martinson DG, McIntyre A, Mix AC, Molfino B, Morley JJ, Peterson LC, Pisias NG, Prell WL, Raymo ME, Shackleton NJ, Toggweiler JR (1993) On the structure and origin of major glaciation cycles 2. The 100,000-year cycle. Paleoceanography 8(6):699–735

Jackson CS, Broccoli AJ (2003) Orbital forcing of Arctic climate: mechanisms of climate response and implications for continental glaciation. Clim Dyn 21:539–557

Jacob R (1997) Low frequency variability in a simulated atmospheric ocean system. PhD thesis, University of Wisconsin-Madison, p 177

Jacob R, Shafer C, Foster I, Tobis M, Anderson J (2001) Computational design and performance of the fast ocean atmosphere model, version one. In: Alexandrov V (ed) Proceedings of the 2001 international conference on computational science, Springer, Heidelberg, pp 175–184

Joussaume S, Braconnot P (1997) Sensitivity of paleoclimate simulation results to season definition. J Geophys Res 102(D2):1943–1956

Kutzbach JE (1981) Monsoon climate of the early Holocene: climate experiment with the earth's orbital parameters for 9000 years ago. Science 214:59–61

Kutzbach JE, Otto-Bliesner BL (1982) The sensitivity of the African–Asian monsoonal climate to orbital parameter changes for 9000 yr B.P. in a low-resolution general circulation model. J Atmos Sci 39(6):1177–1188

Kutzbach JE, Gallimore RG (1988) Sensitivity of a coupled atmosphere/ mixed-layer ocean model to changes in orbital forcing at 9000 yr BP. J Geophys Res 93:803–821

Liu Z, Otto-Bliesner B, Kutzbach J, Li L, Shields C (2003) Coupled climate simulation of the evolution of global monsoons in the Holocene. J Clim 16:2472–2490

Liu Z, Wang Y, Gallimore R, Notaro M, Prentice IC (2006) On the cause of abrupt vegetation collapse in North Africa during the Holocene: climate variability vs. vegetation feedback. Geophys Res Lett 33, L22709, doi: 10.1029/2006GL028062

Lorenz SJ, Lohmann G (2004) Accelerated technique for Milankovitch type forcing in a coupled atmosphere–ocean circulation model: method and application for the Holocene. Clim Dyn 23:727–743

Magee JW, Miller GH, Spooner NA, Questiaux D (2004) Continuous 150 ky monsoon record from Lake Eyre, Australia: insolation forcing implications and unexpected Holocene failure. Geology 32:885–888

Montoya M, von Storch H, Crowley TJ (2000) Climate simulation for 125,000 years ago with a coupled ocean–atmosphere general circulation model. J Clim 13:1057–1072

Morley JJ, Heusser LE (1997) Role of orbital forcing in East Asian monsoon climates during the last 350 kyr: evidence from terrestrial and marine climate proxies from core RC114-99. Paleoceanography 12:483–493

Pokras EM, Mix AC (1987) Earth's precession cycle and quaternary climatic change in tropical Africa. Nature 326:486–487

Prell WL, Kutzbach JE (1992) Sensitivity of the Indian monsoon to forcing parameters and implications for its evolution. Nature 360:647–652

Reichart GJ, Lourens L, Zachariasse WJ (1998) Temporal variability in the northern Arabian Sea oxygen minimum zone (OMZ) during the last 225,000 years. Paleoceanography 13:607–621

Ruddiman WF (2006) What is the timing of orbital-scale monsoon changes? Quaternary Sci Rev 25:657–658

Rossignol-Strick M (1983) African monsoons, an immediate response to orbital insolation. Nature 304:46–49

Short DA, Mengel JG (1986) Tropical climate phase lags and Earth's precession cycle. Nature 323:48–50

Sun J, Huang X (2006) Half-precessional cycles recorded in Chinese loess: response to low-latitude insolation forcing during the last interglacial. Quaternary Sci Rev 25:1065–1072

Timmermann A, Lorenz S, An S-I, Clement A, Xie S-P (2007) The effect of orbital forcing on the mean climate and variability of the tropical Pacific. J Clim (in press)

Tuenter E, Weber SL, Hilgen FJ, Lourens LJ, Ganopolski A (2005) Simulation of climate phase lags in response to precession and

obliquity forcing and the role of vegetation. Clim Dyn 24:279–295

Wang P, Clemens S, Beaufort L, Braconnot P, Ganssen G, Jian Z, Kershaw P, Sarnthein M (2005) Evolution and variability of the Asian monsoon system: state of the art and outstanding issues. Quaternary Sci Rev 24:595–629

Webster PJ (1987) The elementary monsoon. In: Fein JS , Stevens PL (eds) Monsoons. Wiley, New York, pp 3–32

Wyrwoll K-H, Valdes P (2003) Insolation forcing of the Australian monsoon as controls of Pleistocene mega-lake events. Geophys Res Lett 30(24):2279 doi:10.1029/2003GL018486

Yuan D et al. (2004) Timing, duration, and transitions of the last interglacial Asian monsoon. Science 304:575–578

Zabel M, Wagner T, deMenocal PB (2003) Terrigenous signals in sediments of the low-latitude Atlantic-indications to environmental variations during the late quaternary: Part II: lithogenic matter. In: Wefer G et al. (eds) The South Atlantic in the late quaternary: reconstruction of mass budget and current systems. Springer, Berlin, pp 1–23